Journal of Alloys and Compounds 510 (2012) 71–77

Contents lists available at SciVerse ScienceDirect

Journal of Alloys and Compounds

journal homepage: www.elsevier.com/locate/jallcom

Optimization of pulsed TIG cladding process of stellite alloy on carbon steel using RSM

F. Madadi [1], F. Ashrafizadeh, M. Shamanian *

Department of Materials Engineering, Isfahan University of Technology, Isfahan 8415683111, Iran

ARTICLE INFO

Article history:
Received 26 November 2010
Received in revised form 18 August 2011
Accepted 21 August 2011
Available online 26 August 2011

Keywords:
Pulsed GTAW
Cladding
Mathematical models
Design of experiments

ABSTRACT

Stellite 6 is a cobalt-base alloy which is resistant to wear and corrosion and retains these properties at high temperatures. The exceptional wear resistance of Stellite 6 is mainly due to the unique inherent characteristics of the hard carbides dispersed in a Co–Cr alloy matrix. In this study, pulsed tungsten inert gas (TIG) cladding process was carried out to deposit Stellite 6 on plain carbon steel plate. The beneficial effects of this cladding process are low heat input, low distortion, controlled weld bead volume, less hot cracking tendency, less absorption of gases by weld pool and better control of the fusion zone. The dilution effect is a key issue in the quality of cladded layers and, in this regard, the pulsed current tungsten inert gas (PCTIG) was performed to decrease excess heat input and melting of substrate. This paper deals with the investigation of the hardness and dilution ratio by experimental study and mathematical modeling. The experiments were conducted based on four-factor, five-level central composite rotatable design. The second-order regression method was developed to study the correlations. The developed models were checked for their adequacy and significance by ANOVA analysis and confirmation tests were carried out to check the accuracy of predicted values.

1. Introduction

Stellite 6 is a well-known Co–Cr–W–C alloy where chromium provides mechanical strength by formation of solid solution and corrosion resistance through the formation of chromium oxide protective layer. In addition, this element also acts as the chief carbide former during alloy solidification. Tungsten increases the strength of Co–Cr by solid solution strengthening. Stellite 6 has excellent resistance to many forms of wear and corrosion over a wide range of temperatures, attributed to the high volume fraction of carbides and the unusual deformation characteristics imparted by Co-rich matrix. The relatively low stacking fault energy (SFE), which is sufficiently high to conserve fcc structure, is thought to be important as this structure transformed to hcp during processing and service conditions. Stellite 6 has an outstanding resistance to seizing or galling as well as cavitation erosion [1,2] and is extensively used to combat galling in valve trims, pump sleeves and liners.

Hardfacing is a surface modification technology in which a specially designed alloy is surface welded in order to enhance surface properties depending on the characteristics of selected alloys [3,4]. In this process, metallurgical bond forms between the coating and the substrate [5]. The common hardfacing techniques include oxy-acetylene gas welding (OAW), gas tungsten arc welding (GTAW) or tungsten inert gas welding (TIG), submerged arc welding (SAW) and plasma transferred arc welding (PTA). The significant differences between these processes are the welding efficiency and the dilution ratio of cladded layers [6].

GTAW is an arc welding process that utilizes the arc between a non-consumable tungsten electrode and the weld pool. The materials are melted by the intense heat of the arc and fuse together. Once the arc and weld pool are established, the torch is moved along the joint line. The arc progressively melts the base metal and filler metal (Fig. 1). The GTAW process usually produces a superior quality weld and a precise control. In the pulsed-current mode, the welding current rapidly alternates between two levels; the higher current state is known as the pulse current (I_p), while the lower current level is called the background current (I_b). During the period of pulse current, the weld area is heated and fusion occurs and, upon dropping to the background current, the weld area is allowed to cool and solidify.

Pulsed GTAW process parameters are depicted in Fig. 2. The considerable advantage of pulsed-current GTAW is lower heat input which results in diminishing of distortion and warpage in thin work pieces. Using GTAW process, the weld pool and fusion zone, weld penetration, welding speed and weld quality are easily controlled and the absorption of gases by weld pool and hot cracking tendency can be diminished [7,8]. In a continuous current GTAW, heat input is calculated from continuous current while in the pulsed process,

* Corresponding author. Tel.: +98 311 3915737, fax: +98 311 3915737.
E-mail addresses: f.madadi@ma.iut.ac.ir (F. Madadi), shamanian@cc.iut.ac.ir (M. Shamanian).
[1] Tel.: +98 9133038446.

0925-8388/$ – see front matter © 2011 Elsevier B.V. All rights reserved.
doi:10.1016/j.jallcom.2011.08.073

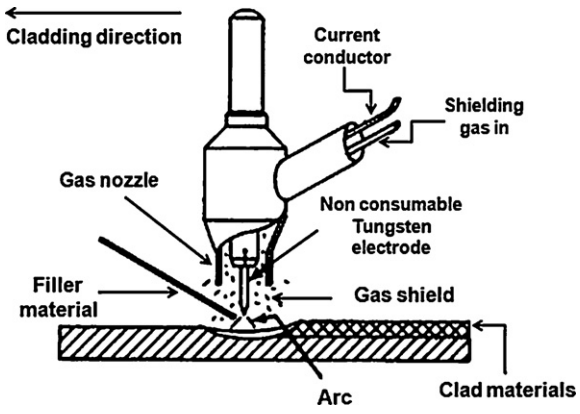

Fig. 1. Schematic of GTA weld cladding.

heat input is calculated from the medium current. The heat input per unit length has a relation with voltage and current as well as reversely proportional to welding speed.

Heat input is considered a very important factor as it affects the bead geometry, dilution and corrosion properties of the clad.

The equation for medium current and heat input (HI) [9] may be written as;

$$Im\,(\mathrm{A}) = \frac{(I_\mathrm{p} \times t_\mathrm{p}) + (I_\mathrm{b} \times t_\mathrm{b})}{t_\mathrm{p} + t_\mathrm{b}} \quad (1)$$

$$\mathrm{HI}\,(\mathrm{kJ/mm}) = \frac{Im \times V}{S} \times \eta \quad (2)$$

where V is voltage, S is welding speed and η is efficiency of GTAW process (usually assumed to be 60–70%) [9].

Extensive research has been performed in pulsed current welding process [10]. Frequently reported metallurgical advantages of pulsed current welding in literature include grain and substructure refinement of the fusion zone and control of segregation [11]. However, published research on the relation between the pulse current parameters and dilution is very scarce. Even though sufficient literature is available on cladding of stellite alloys, no systematic study has been reported so far to correlate the process parameters with dilution and hardness. Hence, in this investigation an attempt was made to develop mathematical models based on four-factor, five-level central composite rotatable design with full replication technique to predict the dilution and hardness of stellite hardfacing

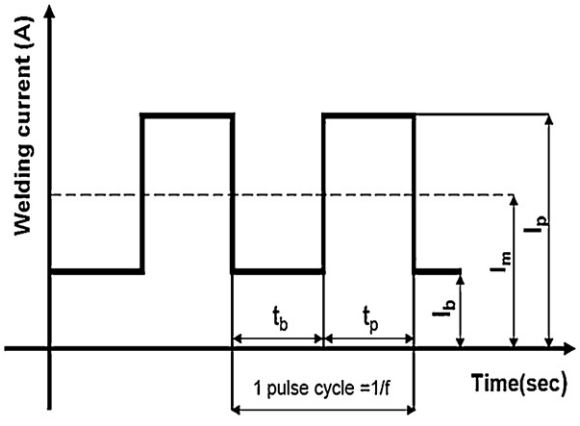

Fig. 2. Pulse GTAW process parameter.

on carbon steel using statistical tools such as design of experiments, analysis of variance and regression analysis. The response surface methodology (RSM), described in this paper, is helpful in developing an approximation for the true functional relationship between the independent variables and the response variable.

2. Design of experiment procedure based on response surface method

Response surface method (RSM) is an important branch of experimental design used in development of new processes and optimization of their performance [12]. As an important subject in the statistical design of experiments, RSM is a collection of mathematical and statistical techniques useful for the modeling and analysis of problems. In the RSM procedure, a response of interest is influenced by several variables and objective which should optimize this response. According to Hill and Hunter [13], RSM was introduced in 1951. RSMs are designs and models for working with continuous treatments when finding the optimum condition or description of the response is the goal. When the number of responses is more than one, it is important to find the compromised factor optimizing more than one response. When there are constraints on the design data, then the experimental design has to meet requirements of the constraints. The second goal is to understand how the response is changed in a given direction by adjusting the design variables. After finding the upper and lower limits (i.e. range) of the identified process parameters, the experiments are conducted as per the selected the experimental design matrix. The second-order regression mathematical model has been developed to predict responses [13,14].

2.1. Determination of the important process parameters

The properties of the clad materials such as mechanical strength are influenced not only by the chemical composition but also by the clad dilution [10]. The acceptable clad dilution depends on heat input and the heat input, in turn, depends on welding current, arc voltage, etc. Therefore, weld cladding can be considered as a multi input, multi-output process. A common problem of the manufacturers is the control of the process input parameters to obtain a good clad together with the required quality of the surface with minimal detrimental residual stresses and dilution. In order to find a correlation between input and responses and minimize the error, various optimization methods can be applied to define the desired output variables through developing mathematical models [15]. The process parameters were selected based on the results of several preliminary experiments and the data obtained from literature [16–18]. These parameters include peak current, base current, pulse frequency and pulse on time. The chosen process parameters were peak current, base current, pulse frequency and pulse on time.

2.2. Working ranges of process parameters and design of experiment

A large number of trials have been conducted by variation of one of the process parameters and keeping the others constant. The working range of peak current, base current, pulse frequency and pulse on time have been explored by inspection of bead appearance, clad quality and the absence of visible defects such as surface porosity, undercut, etc. In this regard the constant process parameters and the selected pulsed GTAW process variables and their levels are presented in Tables 1 and 2, respectively. Due to the wide range of variables a central composite rotatable full factorial experimental design with four-factors and five-levels was selected to conduct the experiments and optimize the condition. The experimental design consisted of 31 runs that are shown in Table 3. In this matrix, first 16

Table 1
Constant process parameter.

Process parameter	Constant value
Shielding gas flow rate, 1/min	10
Purging gas flow rate, 1/min	5
Filler rod diameter, mm	2
Electrode material	98% W + 2% Zr
Electrode diameter, mm	3.15
Mean arc voltage, V	14

rows represent the full factorial ($2^4 = 16$) design and next eight rows show the star point and last seven rows exhibit the center point. The distance of the axial runs from the center is defined as α. The choice of α is crucial to the performance of the design. To maintain rotatability, the value of α should depend on the number of experimental runs in the factorial portion of the central composite design [19]:

$$\alpha = [\text{number of factorial runs}]^{1/4}$$

If the factorial is a full factorial, then:

$$\alpha = [2^k]^{1/4}$$

where k is number of factor. (e.g. for four-factor, $\alpha = 2^{4/4} = 2$).

All parameters were coded as (0) related to the center points. In addition, the combinations of each parameter and its highest or lowest value were coded as (+2) or (−2). The combinations of each parameter with other three parameters of the middle levels (0) established the star points [20].

The limit of each variable was restricted to highest value (+2) and lowest value (−2). The coded values for middle values can be calculated using the following equation.

$$X_i = \frac{2[2X - (X_{max} + X_{min})]}{X_{max} - X_{min}} \quad (3)$$

where X_i is the required coded value of a parameter X. X is any value of the parameter from X_{min} to X_{max}, X_{min} is the lower limit of the parameter and X_{max} is the upper limit of the parameter.

2.3. Experimental procedure

In this study, plain carbon steel (DIN1.0570 or St52) was used as the substrate. Stellite 6 wires (diameter: 2 mm) were used as cladding materials. The chemical composition of clad material is shown in Table 4.

Prior to cladding, the base metal sheets were wire brushed, and degreased using acetone and finally preheated to 100 °C. The argon gas was used for shielding. The weld joint was completed in single pass to minimize the excess heat input.

Table 2
Working range of process parameter.

Symbol	Process parameter	Unit	Notation	Level coded				
				(−2)	(−1)	(0)	(+1)	(+2)
1	Peak current	A	*P*	80	90	100	110	120
2	Base current	A	*B*	40	50	60	0	80
3	Frequency	Hz	*F*	0	3	6	9	12
4	On time	%	*T*	35%	40%	45%	50%	55%

Table 3
Design of experiment and responses.

Experiment no.	*P*(*X*1)	*B*(*X*2)	*F*(*X*3)	*T*(*X*4)	Hardness (VHN)	Dilution (%)
1	−1	−1	−1	−1	365	28.5
2	1	−1	−1	−1	355	33.7
3	−1	1	−1	−1	360	31.6
4	1	1	−1	−1	320	37.8
5	−1	−1	1	−1	380	25.4
6	1	−1	1	−1	340	30.5
7	−1	1	1	−1	350	29.5
8	1	1	1	−1	330	35.8
9	−1	−1	−1	1	380	27
10	1	−1	−1	1	350	30.5
11	−1	1	−1	1	395	22.25
12	1	1	−1	1	330	37
13	−1	−1	1	1	390	23.3
14	1	−1	1	1	340	32
15	−1	1	1	1	380	24.8
16	1	1	1	1	360	30.3
17	−2	0	0	0	405	20.16
18	2	0	0	0	325	38
19	0	−2	0	0	400	21.2
20	0	2	0	0	480	25.3
21	0	0	−2	0	305	41
22	0	0	2	0	340	31.5
23	0	0	0	−2	410	20.5
24	0	0	0	2	400	21
25	0	0	0	0	405	21
26	0	0	0	0	410	18.5
27	0	0	0	0	415	18
28	0	0	0	0	430	15
29	0	0	0	0	425	16
30	0	0	0	0	400	19.5
31	0	0	0	0	420	17.04

Table 4
The chemical composition (wt%) of clad material.

Elements	Cr	W	Ni	C	Si	Mn	Fe	Mo	Co
wt%	28.6	4.9	2.2	1.3	1.1	0.3	1.9	<0.1	Bal

2.4. Recording the response variables

At first, the specimens were prepared for metallographic observation and microhardness tests. In this regard, the transverse sections of each weld overlay were cut from midlength position of all clad samples. Aqua solution ($3HCl{:}1HNO_3$) was used for metallographic studies and revelation of the bead profiles. Some of the specimens prepared for dilution measurement are displayed in Fig. 3. As mentioned before, dilution is a determining factor for assessment of coating properties. Dilution values obtained from the different experiment conditions are presented in Table 3. Regarding the influence of the substrate material on the measured dilution, results which vary with the current intensity were used. Dilution was evaluated as the area ratio between the substrate melted area and total melted area and the percentage of dilution was individually calculated using the following equation [21];

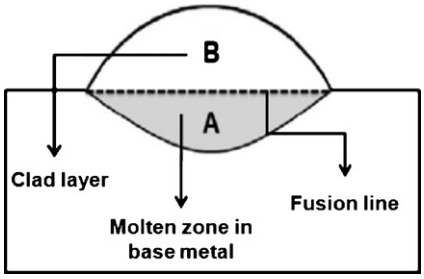

$$\text{Dilution } (\%) = \frac{A}{A+B} \times 100 \tag{4}$$

Microhardness measurements were carried out on the cladded samples at a load of 100 g and dwell time of 15 s using a Vickers digital microhardness tester (BUEHLER).

The microhardness values corresponding to the lowest and highest amounts of dilution (experiment number 28 and 21, respectively) are shown in Fig. 4.

3. Development of mathematical model

A procedure based on regression was used for the development of mathematical models and to predict the clad hardness and dilution [22].

The second-order model includes all the terms in the first-order model, plus all quadratic terms like $\beta_{11} X_{1i}^2$ and all cross product terms like $\beta_{13} X_{1i} X_{3j}$. The response surface function representing dilution can be expressed as following equation:

$$D = f\ (\textit{peak current}, \textit{base current}, \textit{pulse frequency}, \textit{pulse on time})$$
$$= f(P, B, F, T) \tag{5}$$

The second-order response surface model [23] for the four-factors is given by Eq. (6)

$$D = \beta_0 + \sum_{i=1}^{4} \beta_i X_i + \sum_{i=1}^{4} \beta_{ii} X_i^2 + \sum_{\substack{i=1 \\ i<j}}^{4} \beta_{ij} X_i X_j + \varepsilon \tag{6}$$

where β_0 is a constant term of the regression equation, the coefficient β_i is linear terms, the coefficient β_{ii} is the quadratic terms, and the coefficient β_{ij} is the interaction terms and $\varepsilon \sim N(0,\sigma^2)$.

All the co-efficient were calculated for their significance at 95% confidence level applying Minitab15 statistical software package.

The results of analysis of variance for two responses are given in Tables 5 and 6.

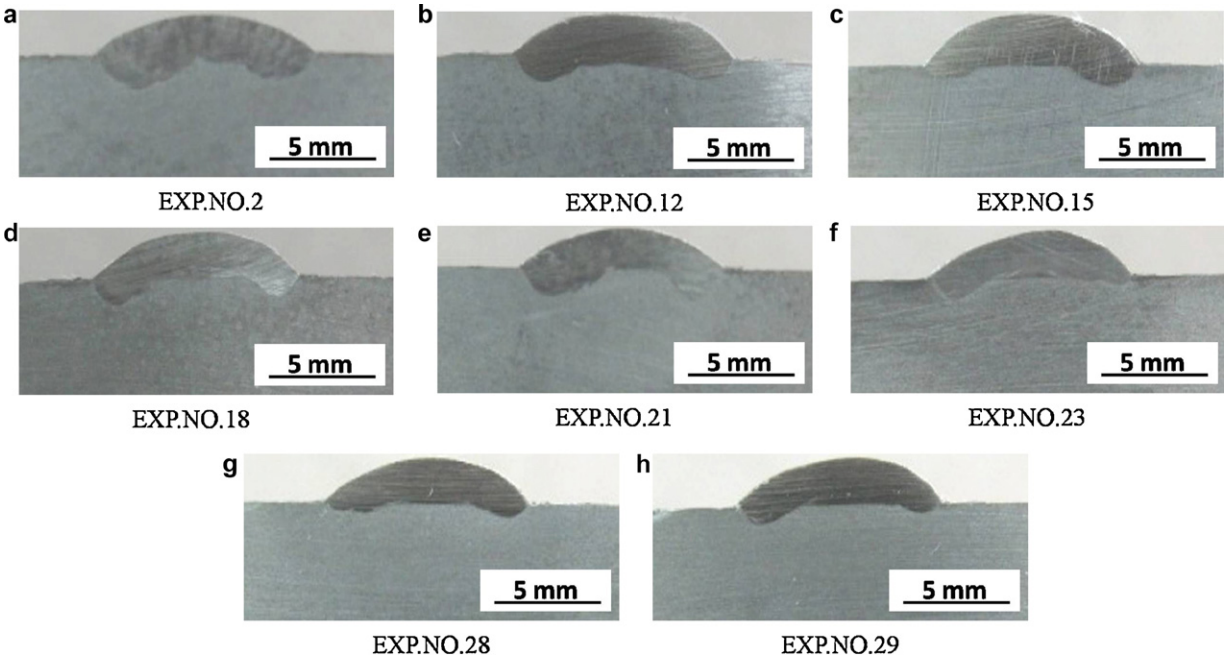

Fig. 3. Cross section image of some of specimens.

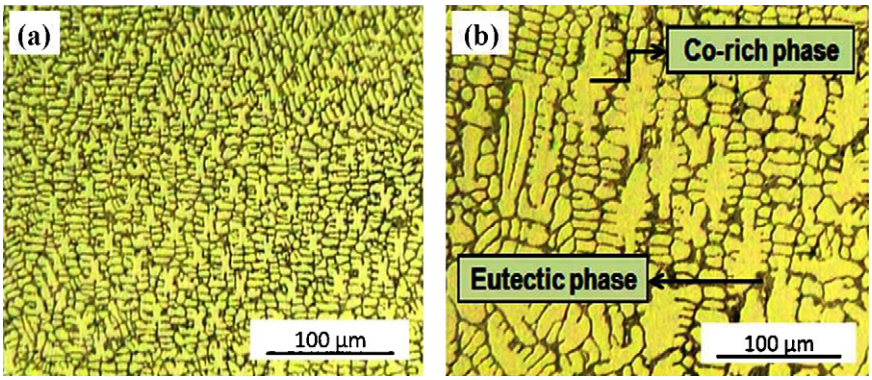

Fig. 4. Microstructure of the specimens with (a) lowest and (b) highest amounts of dilution.

Table 5
ANOVA result for hardness.

Term	Coef	SE Coef	*T*	*P*
Constant	415	5.45	74.841	0.000
P	−18.125	2.995	−6.052	0.000
B	−4.792	2.955	−1.600	0.129
F	3.542	2.955	1.183	0.254
T	4.375	2.955	1.461	0.163
P × *P*	−14.635	2.744	−5.335	0.000
B × *B*	−8.385	2.744	−3.056	0.008
F × *F*	−25.260	2.744	−9.207	0.000
T × *T*	−4.635	2.744	−1.690	0.110
P × *B*	−0.938	3.668	−0.256	0.802
B × *F*	0.937	3.688	0.256	0.802
P × *T*	−3.438	3.688	−0.937	0.363
B × *F*	0.938	3.688	0.256	0.802
B × *T*	5.313	3.688	1.488	0.167
F × *T*	0.938	3.688	0.256	0.802

Table 6
ANOVA result for dilution.

Term	Coef	SE Coef	*T*	*P*
Constant	17.8629	1.0535	16.956	0.000
P	3.7887	0.5689	6.659	0.000
B	1.0979	0.5689	1.930	0.072
F	−1.4896	0.5689	−2.618	0.019
T	−1.0271	0.5689	−1.805	0.090
P × *P*	3.2483	0.5212	6.232	0.000
B × *B*	1.7908	0.5212	3.436	0.003
F × *F*	5.0408	0.5212	9.671	0.000
T × *T*	1.1658	0.5212	2.237	0.040
P × *B*	0.6406	0.6968	0.919	0.372
B × *F*	−0.2531	0.6968	−0.363	0.721
P × *T*	0.6031	0.6968	0.866	0.400
B × *F*	0.0156	0.6968	0.022	0.982
B × *T*	−0.9406	0.6968	−1.350	0.196
F × *T*	0.2531	0.6968	0.363	0.721

According to the ANOVA results, after determination of the significant coefficients, mathematical models were developed by using these coefficients only after elimination of the insignificant coefficients. The developed models with welding parameters in coded form are given below:

$$D\% = 17.8629 + 3.78875P + 1.0992B - 1.48958F + 3.24835P^2 + 1.79085B^2 + 5.04085F^2 + 1.16585T^2 \quad (7)$$

$$H = 415.008 - 18.125P - 14.64P^2 - 8.39B^2 - 25.265F^2 \quad (8)$$

Cladding with stellite is commonly used to produce surface layers for wear, corrosion and oxidation resistance at high temperatures. As the substrate melts, it is mixed with the stellite clad layer which resulted in dilution of clad layer. Consequently, the composition of clad layer is changed near the interfacial regions. The extent of dilution is proportional to the arc current and, as indicated by Eq. (2), it increases with the heat input of the welding process. At low current values, the heat input is not enough to melt the substrate. Therefore, the dilution of clad layer will be diminished. When higher arc current values are employed, the depth of penetration is increased which leads to increase in dilution.

Another important factor is the pulse duty cycle which is defined as the time between peak value and base value in pulsed current welding process. The effect of this factor on dilution is similar to that of arc current. As the pulse frequency increases, the penetration depth and dilution increase. Consequently, the hardness of the cladding layer decreases.

3.1. Checking the adequacy of the developed models

The adequacy of the developed models was checked using the analysis of variance technique [24,25]. This includes:

(a) The results of the ANOVA (Tables 7 and 8) show that the regression is significant with linear and quadratic terms for both models (*p*-value is less than 0.05):

Table 7
ANOVA results for testing adequacy of the hardness models.

Source	df	Seq SS	Adj SS	Adj MS	*F*	*P*
Regression	14	32877.2	32877.2	2348.4	10.91	0.000
Linear	4	9195.8	9195.8	2299.0	10.68	0.000
Square	4	22984.5	22984.8	5746.1	26.70	0.000
Interaction	6	696.9	696.9	116.1	0.54	0.771
Residual Error	16	3443.7	3443.7	215.2		
Lack of Fit	10	2743.8	2743.8	274.4	2.35	0.154
Pure Error	6	700.0	700.0	116.7		
Total	30	36321.0				

SS: sum of square; MS: mean square; df: degree of freedom.

Table 8
ANOVA results for testing adequacy of the dilution models.

	df	Seq SS	Adj SS	Adj MS	*F*	*P*
Regression	14	1451.14	1451.14	103.653	13.34	0.000
Linear	4	452.01	452.01	113.003	14.55	0.000
Square	4	970.53	970.53	242.632	31.23	0.000
Interaction	6	28.60	28.60	4.766	0.61	0.717
Residual error	16	124.30	124.30	7.769		
Lack of fit	10	99.01	99.01	9.901	2.35	0.154
Pure error	6	25.29	25.29	4.215		
Total	30	1575.44				

SS: sum of square; MS: mean square; df: degree of freedom.

(b) The validity of the model was checked by residual plots for each response as shown in Figs. 5 and 6.

Finally, the scatter diagrams were drawn showing the degree of closeness between observed and predicted values of weld bead dimensions. Fig. 7 shows the observed and predicted values of dilution.

Other evidence which indicates high correlation between experimental values and predicted values of hardness and dilution is the value of "R^2" for the above models which is 90.52% and 92.11% for hardness and dilution, respectively.

The values of adjusted square multiple *R* and standard error of estimate for both the full and reduced models are given in Table 9. In comparison to full models, the reduced models have higher values

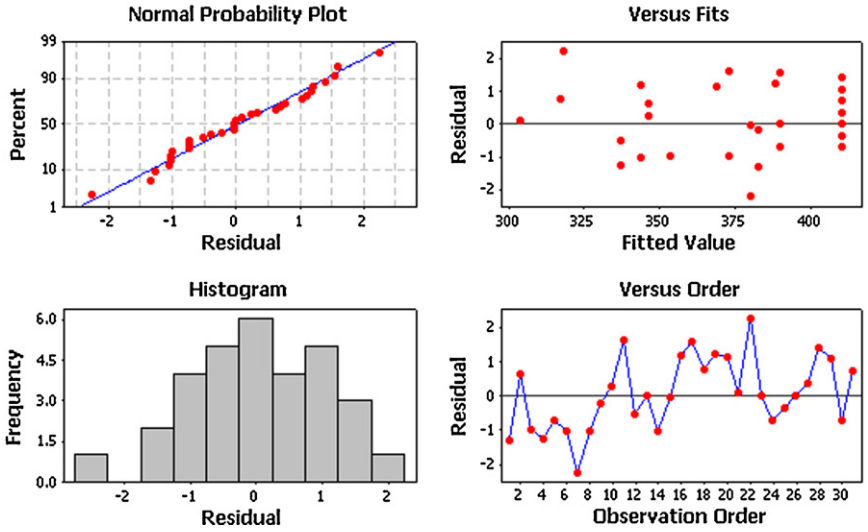

Fig. 5. Residual plots of hardness.

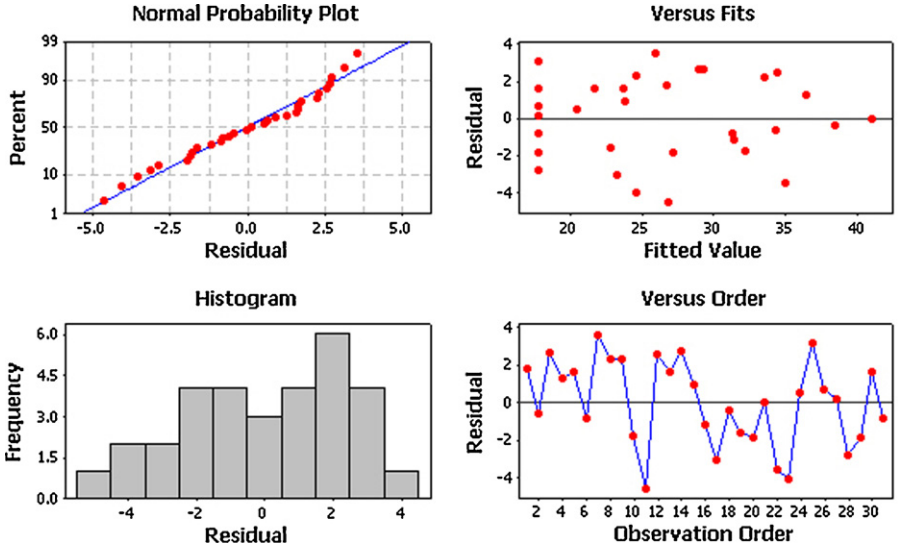

Fig. 6. Residual plots of dilution.

Table 9
Comparison of square multiple "*R*" values and standard error of estimate for full and reduced models.

Source	Adjusted square multiple *R*		Standard error of estimate	
	Full model	Reduced model	Full model	Reduced model
Dilution	0.852	0.867	0.278	0.263
Hardness	0.822	0.855	0.146	0.132

Table 10
Results of conformity test for dilution and hardness.

Test no	Process parameter				Dilution			Hardness		
	I_p	I_b	fr	Time	Predicted values	Observed values	Error (%)	Predicted values	Observed values	Error (%)
1	87	60	7.8	53.5	23.353	24.38	4.594	400.5	392	−2.122
2	96	74	6.3	52	22.538	23.35	3.602	406.232	395	−2.764
3	100	60	6	45	17.86	18.5	3.459	415.008	410	−1.206
Mean error							3.885			−2.03

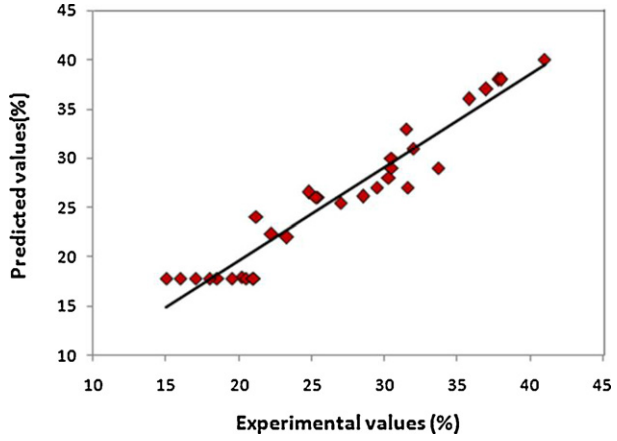

Fig. 7. Scatter diagram for the response dilution.

of R^2 and lower values of standard error (Table 9). Therefore, the reduced models are preferred to the full models.

4. Conformity test to declare of mathematical model validity

Conformity tests were carried out with the same experimental conditions to validate the adequacy of the mathematical models correlation. The results of the conformity test are presented in Table 10. From the results of conformity test, it is found that non-linear regression model is able to predict dilution and hardness with acceptable accuracy.

The error percentage was then calculated as;

$$\text{Error}\ \ (\%) = \frac{\text{observed}\ \ \text{values} - \text{predicted}\ \ \text{values}}{\text{predicted}\ \ \text{values}}$$

5. Conclusions

This paper has described the use of design of experiments (DOE) for conducting experiments. From this investigation, the following conclusions are derived:

- This study is useful to optimize the welding process variables in order to control the heat input and cooling rates such that the hardness and dilution of the clad could be estimated.
- Central composite rotatable design technique with five-level, four-factor full-factorial design matrix and mathematical models was used to predict hardness and dilution of pulsed gas tungsten arc weld cladding of Stellite 6 on carbon steel with high accuracy.
- The results predicted by mathematical models were close to those obtained by experiments. The confirmation tests also indicated high correlation between the mentioned values.
- All of the chosen pulse GTAW parameters were significant and showed a noticeable influence on clad dilution.
- The welding current is an effective parameter affecting heat input and melting. In this regard, it is the most important process parameter which influences the dilution. Increase in welding current leads to increase in dilution percentage and vice versa.

References

[1] K.C. Antony, W.L. Silience, Proceedings of the Fifth International Conference on Erosion by Solid and Liquid Impact, Cambridge University Press, 1979, p. 631.
[2] K.J. Bhansali, A.E. Miller, ASME (1982) 179.
[3] J.R. Davis, Davis and Associates, ASM Handbook-–Welding, Brazing and Soldering, vol. 6, 10th ed., ASM Metals Park, OH, 1993, pp. 699–828.
[4] E. Lugscheider, U. Morkramer, A. Ait-Mekideche, Proceedings of the Fourth National Thermal Spray Conference, Pittsburgh, PA, USA, 1991.
[5] A.K. Jha, B.K. Prasad, R. Dasgupta, O.P. Modi, J. Mater. Eng. Perform. 8 (1999) 190.
[6] S. Kumar, D.P. Mondal, H.K. Khaira, A.K. Jha, J. Mater. Eng. Perform. 8 (1999) 711.
[7] K. Weman, Welding Processes Handbook, CRC Press LLC, New York, 2003.
[8] H.B. Cary, S.C. Helzer, Modern Welding Technology, Pearson Education, Upper Saddle River, New Jersey, 2005.
[9] J. Cornu, Advanced Welding System, TIG and Related Processes, vol. 3, Springer, Heidelberg, 1988, p. 61.
[10] A.S.C.M. D'Oliveira, R.S.C. Paredes, R.L.C. Santos, J. Mater. Process. Technol. 171 (2006) 167–174.
[11] F. Madadi, M. Shamanian, F. Ashrafizadeh, Surf. Coat. Technol. 205 (2011) 4320–4328.
[12] G.E.P. Box, J.S. Hunter, Ann. Math. Stat. 28 (1957) 195–241.
[13] G.E.P. Box, K.B. Wilson, J. Roy. Stat. Soc. B 13 (1951) 1–45.
[14] A.I. Khuri, J.A. Cornell, Design and Analysis, Marcel Dekker, New York, 1996.
[15] K.Y. Benyounis, A.G. Olabi, Adv. Eng. Softw. 39 (2008) 483–496.
[16] C.F. Tseng, W.F. Savage, Weld. J. 50 (1971) 777–786.
[17] M. Balasubramanian, V. Jayabalan, V. Balasubramanian, J. Mater. Process. Technol. 196 (2008) 222–229.
[18] D.W. Becker, C.M. Adams Jr., Weld. J. 57 (1978) 134–138.
[19] J.W. Wealleans, B. Allen, Weld. Met. Fabr. 37 (1969) 210–213.
[20] D.C. Montgomery, Design and Analysis of Experiments, vol. 3, John Wiley and Sons, New York, 1991.
[21] A.S.C.M. D'Oliveira, R. Vilar, C.G. Feder, Appl. Surf. Sci. 201 (2002) 154–160.
[22] T.B. Barker, Quality by Experimental Design, ASQC Quality Press: Marcel Dekker, 1985.
[23] W. Kurz, D.J. Fischer, Fundamentals of Solidification, Trans Tech Publications, Aedermannsdorf, 1992.
[24] V. Gunaraj, N. Murugan, J. Mater. Process. Technol. 95 (1999) 246–261.
[25] N. Murugan, R.S. Parmar, Intern. J. Join. Mater. 7 (1995) 71–80.